# Direct Synthesis of Mesoionic Carbene (MIC) Stabilized Gold Nanoparticles from 1,2,3-Triazolium Salts

Alexandre Porcheron,[a,b]‡ Omar Sadek,[b]‡ Salem Ba Sowid,[a,b]‡ Nathalie Bridonneau,[a] Laura Hippolyte,[a,b] Dimitri Mercier,[c] Philippe Marcus,[c] Clément Chauvier,[b] Corinne Chanéac,[a] Louis Fensterbank,*[b] François Ribot*[a]

[a] Dr. A. Porcheron, S. B. Sowid, Dr. N. Bridonneau, Dr. L. Hippolyte, Prof. C. Chanéac, Dr. F. Ribot
Sorbonne Université, CNRS, Laboratoire de Chimie de la Matière Condensée de Paris (LCMCP), F-75252 Paris Cedex 05, France.
E-mail: francois.ribot@sorbonne-universite.fr

[b] Dr. A. Porcheron, Dr. O. Sadek, S. B. Sowid, Dr. L. Hippolyte, Dr. C. Chauvier, Prof. L. Fensterbank
Sorbonne Université, CNRS, Institut Parisien De Chimie Moléculaire (IPCM), F-75252 Paris Cedex 05, France.
E-mail: louis.fensterbank@sorbonne-universite.fr

[c] Dr. D. Mercier, Prof. P. Marcus
PSL Research University, CNRS – Chimie ParisTech, Institut de Recherche de Chimie Paris, Physical Chemistry of Surfaces Research Group, Paris, France

‡These authors contributed equally to this work

**Abstract:**
Significant achievements have been reported in the last few years regarding the stabilization and functionalisation of gold nanoparticles (AuNPs), mainly through the use of thiols and imidazolylidene N-heterocyclic carbenes capping ligands. Herein, we report that mesoionic carbenes (MICs) ligands, based on the 1,2,3-triazol-5-ylidene scaffold, allow the expeditive preparation of AuNPs of exceptional stability through a simple and straightforward one-pot protocol directly from triazolium salts and discrete Au(III) sources. Control over the size of the AuNPs has been achieved by varying the Au/ligand ratio as well as the nature of the triazolium salts, the latter being facilitated by the ease of synthesis of the MIC precursors through click chemistry. Characterisation of these MIC-AuNPs by X-ray photoelectron spectroscopy (XPS) hints at the exclusive presence of MICs on the nanoparticle surface.

**Introduction:**

Nanoparticles are one of the main pillars on which nanotechnologies have been flourishing over the last decades. The significant surface-to-mass ratio and peculiar properties that matter can exhibit at such a scale constitute the central motivations of academic and industrial interest in nanoparticles.[1] Gold nanoparticles (AuNPs), due to their plasmonic properties and various applications, are one of the most studied systems.[2] They form a fertile ground for the design of novel applications in the fields of medicine, biosensors, or catalysis.[3] In this context, expanding the toolbox available to synthesize stable AuNPs, with control of size and properties, is a topic of intense research interest.

AuNPs require surface ligands to kinetically protect them from irreversible aggregation, in addition to providing the desired functionalisation for targeted applications. Over the last decade, N-heterocyclic carbenes have emerged as a promising family of surface ligands.[4] These ligands, which possess a formally divalent carbon atom, are able to form strong covalent bonds with surface metal atoms. For example, (benz)imidazolinium based NHCs were shown to be excellent ligands for the functionalisation of gold surfaces, demonstrating stability under harsh acidic conditions.[5] Cyclic (alkyl)(amino)carbene (CAACs) were also recently successfully deposited on gold surfaces.[6]

NHCs based on the 1,3-imidazol-2-ylidene scaffold[7] (ImNHC) have received significant attention mainly owing to the stability they impart to surfaces and to their relative ease of preparation and handling.[4] Stable ImNHC-stabilized AuNPs were seminally prepared by ligand exchange in a top-down approach by Fairlamb and Chechik[8], while Tilley[9] employed a bottom-up approach by reducing ImNHC-Au(I) halide complexes (Figure 1). Capitalizing on these studies, many groups have studied the synthesis and properties of NHC stabilized AuNPs,[10] which often display high colloidal stability even under harsh conditions (acidic and basic media, high and low temperatures, salinity), a point of paramount importance in many applications. Nevertheless, these ImNHC platforms are quite inflexible when non-$C_2$-symmetrical or multi-functional species are desired, requiring tedious multi-step syntheses.

Recently, Chin and Reithofer introduced nitrogen acyclic carbenes (NACs) (Figure 1) in an effort to increase the diversity of carbenic ligands able to stabilize AuNPs.[11] NAC-ligated AuNPs stable to thiol exchange were obtained, though the need to handle isocyanide derivatives somewhat limits the possibility of diversification.

Alternatively, mesoionic carbenes (MICs), based on the 1,2,3-triazol-5-ylidene scaffold, offer excellent modularity and facile access to a diverse pool of potential ligands. Their preparation relies on the highly versatile copper-catalyzed alkyne-azide click (CuAAC) reaction,[12] and the quaternarization of the γ-nitrogen ($N^3$), thereby allowing the introduction of up to three distinct substituents on the MIC core. Moreover, MICs are known to be stronger σ-donors than ImNHCs,[13] which should result in stronger coordination to surface atoms. While the potential of MICs in the field of metallic nanoparticles and surfaces was acknowledged in the literature in 2018,[14] it has since remained unexplored. The use of MICs as viable ligands for the stabilization of AuNPs was only very recently reported by Nazemi.[15] Using a bottom-up approach with polymeric MIC-Au(I) iodide complexes, water-soluble AuNPs stable under various conditions, including the presence of exogenous thiols (Figure 1), were prepared, and applied in catalysis.

Building on our long-standing interest and sustained research activity in the synthesis of MIC stabilized gold nanoparticles (MIC-AuNPs),[16] we herein report an alternative simpler synthesis, which directly uses various 1,2,3-triazolium salts and

tetrachloroauric acid to prepare MIC-AuNPs (Figure 1). The procedure is practically simple and does not require the isolation of the Au(I)-carbene precursor prior to AuNP formation.

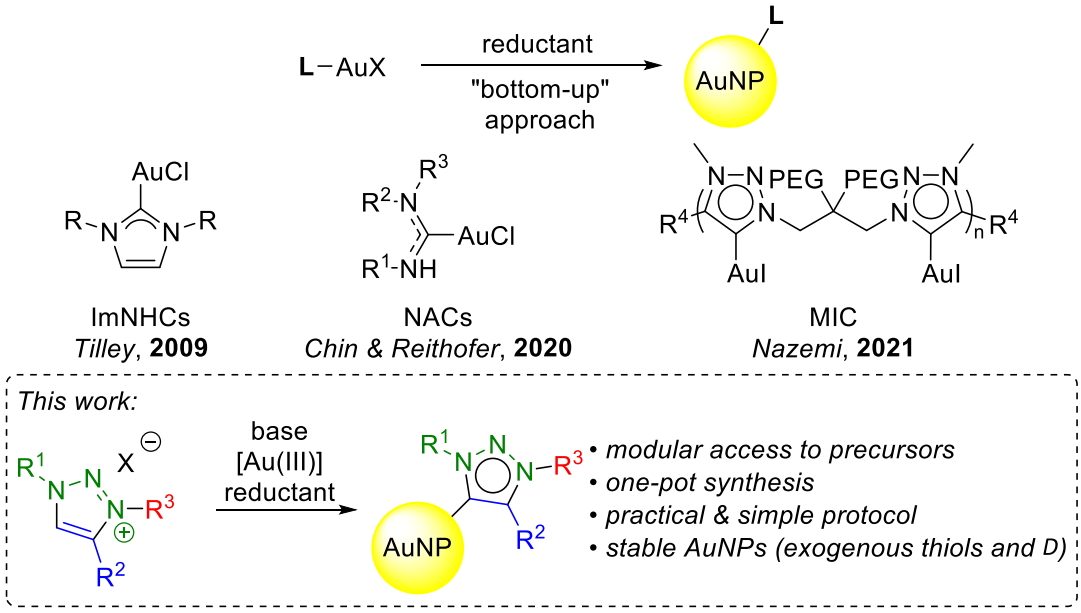


**Figure 1.** NHC-, NAC- and MIC-Au(I) complexes for NHC-, NAC- and MIC-AuNPs synthesis (from literature) and synthesis and stabilization of MIC-AuNPs from triazolium salts (this work).

## Results and Discussion

### Synthesis of triazolium salt precursors

Our synthesis began with a click CuAAC reaction to provide the corresponding 1,2,3-triazole **1** in moderate to good yields (Scheme 1). Given the importance of steric character in NHC-stabilized AuNPs, alkynes and azides of various substitution were chosen to provide triazoles with long ($C_{12}H_{25}$), short ($C_6H_{13}$) and mixed (benzyl) lateral chains. This would allow us to evaluate the effect and limits of such MIC ligands on the stabilization of the derived AuNPs. With these derivatives in hand, facile quaternization of $N^3$ with an alkyl bromide in MeCN at 85 °C provided the corresponding triazolium bromide salts **2** in good to excellent yields. Anion metathesis was performed on **2a** to provide the triazolium hexafluorophosphate **2a-PF$_6$** to investigate the effect of the counterion on nanoparticle synthesis. This was also applied to synthesise **2h-PF$_6$**, as the bromide salt **2h** could not be obtained in pure form.

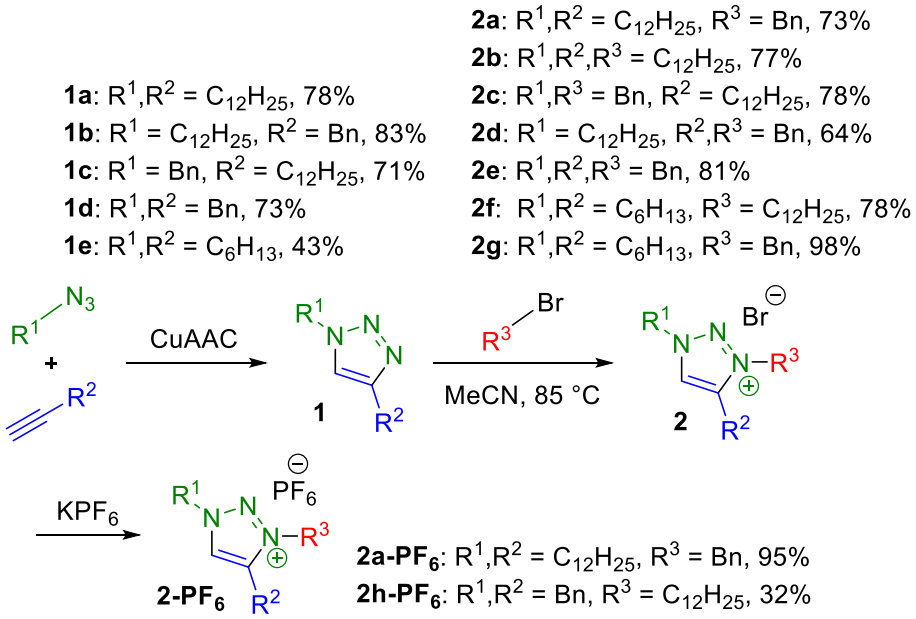


**Scheme 1.** Synthesis of 1,2,3-triazolium salts **2** from 1,2,3-triazoles **1**. Bn = benzyl.

## Synthesis of MIC-AuNPs

Seeking to develop a versatile and streamlined platform for the synthesis of MIC-AuNPs, we designed and optimized our protocol to allow the direct reduction of a gold precursor in the presence of triazolium salt MIC-precursors (Scheme 2). This methodology presents several advantages. Firstly, this avoids the requirement to synthesize, isolate and purify the corresponding MIC-Au(I) halide complex. Secondly, the Au/ligand ratio is not limited to 1:1, as when using MIC-Au(I) complexes, and can be varied. This opens the possibility to tune the size of the MIC-AuNPs, as we have previously demonstrated with NHC-AuNPs.[17]

Practically, the protocol is relatively straightforward: the triazolium precursor **2** is premixed with NaH followed by the Au(III) precursor prior to the addition of $NaBH_4$ as the reducing agent. Addition of $NaBH_4$ causes a colour change from clear yellow/orange to dark burgundy/red, which is highly indicative of gold reduction and AuNP formation. Following reaction work-up, MIC-AuNPs are precipitated from $CH_2Cl_2$ with ethanol and collected by centrifugation. The obtained MIC-AuNPs were characterised by UV/Vis spectroscopy, transmission electron microscopy (TEM) and, for selected examples, by X-ray photoelectron spectroscopy (XPS).

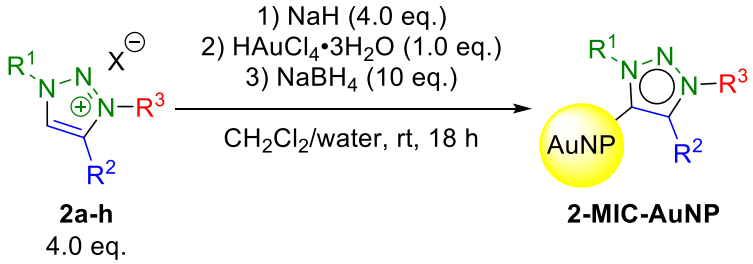


**Scheme 2.** Synthesis of **2-MIC-AuNPs**.

Almost all triazolium salts **2** allowed the isolation of spherical MIC-AuNPs that proved stable for months in suspension in $CH_2Cl_2$ (Figure 2 and Table 1). All isolated MIC-AuNPs displayed a plasmon resonance band (PRB) in the UV/Vis spectrum in the range of 517 – 529 nm (Table 1). As expected, the long alkyl chains ($C_{12}H_{25}$) at the lateral positions ($N^1$ and $C^4$) of **2a** and **2b** allowed the synthesis and isolation of stable and spheroidal AuNPs of 3.2 ± 0.6 and 3.0 ± 0.6 nm for **2a-MIC-AuNP** and **2b-MIC-AuNP**, respectively (Figure 2 a and b). 'Unsymmetrically' substituted triazolium salts **2c** and **2d**, with lateral benzyl and dodecyl substituents, also allow the isolation of stable MIC-AuNPs of 2.8 ± 0.5 and 3.2 ± 0.8 nm for **2c-MIC-AuNP** and **2d-MIC-AuNp**, respectively (Figure 2 c and d). Intriguingly, triazolium salt **2e**, with two flanking benzyl substituents, also allowed the isolation of stable MIC-AuNPs of 3.2 ± 0.8 nm for **2e-MIC-AuNP** (Figure 2 e). However, while triazolium salts **2f** and **2g**, with short $C_6H_{13}$ alkyl chains, did allow the formation of AuNPs as observed by the formation of a dark red solution during the reaction, stable AuNPs could not be isolated as they irreversibly precipitated during the purification process. Similar issues for NP stabilization have been observed when using NHCs with short lateral chains.[10a] Accordingly, for all the triazolium bromide salts used, that yield stable nanoparticles (**2a** to **2e**), sizes around 3 nm with a polydispersity index of 20-25% are obtained when 4 equivalents are introduced in the synthesis.

Interestingly, when triazolium **2a** is associated with a $PF_6$ counterion instead of Br, the nanoparticles obtained are almost 2 nm larger as **2a-$PF_6$-MIC-AuNPs** were found to be 5.1 ± 0.8 nm in size as observed by TEM (Figure 2 f). This counterion effect seems even more pronounced with triazolium salts having flanking benzyl groups on $N^1$ and $C^4$. Indeed, **2h-$PF_6$** provided **2h-$PF_6$-MIC-AuNP**, with a size of 7.4 ± 1.8 nm, while **2e-MIC-AuNP** exhibits a size of only 3.2 ± 0.8 nm (Figure 2 e and g).

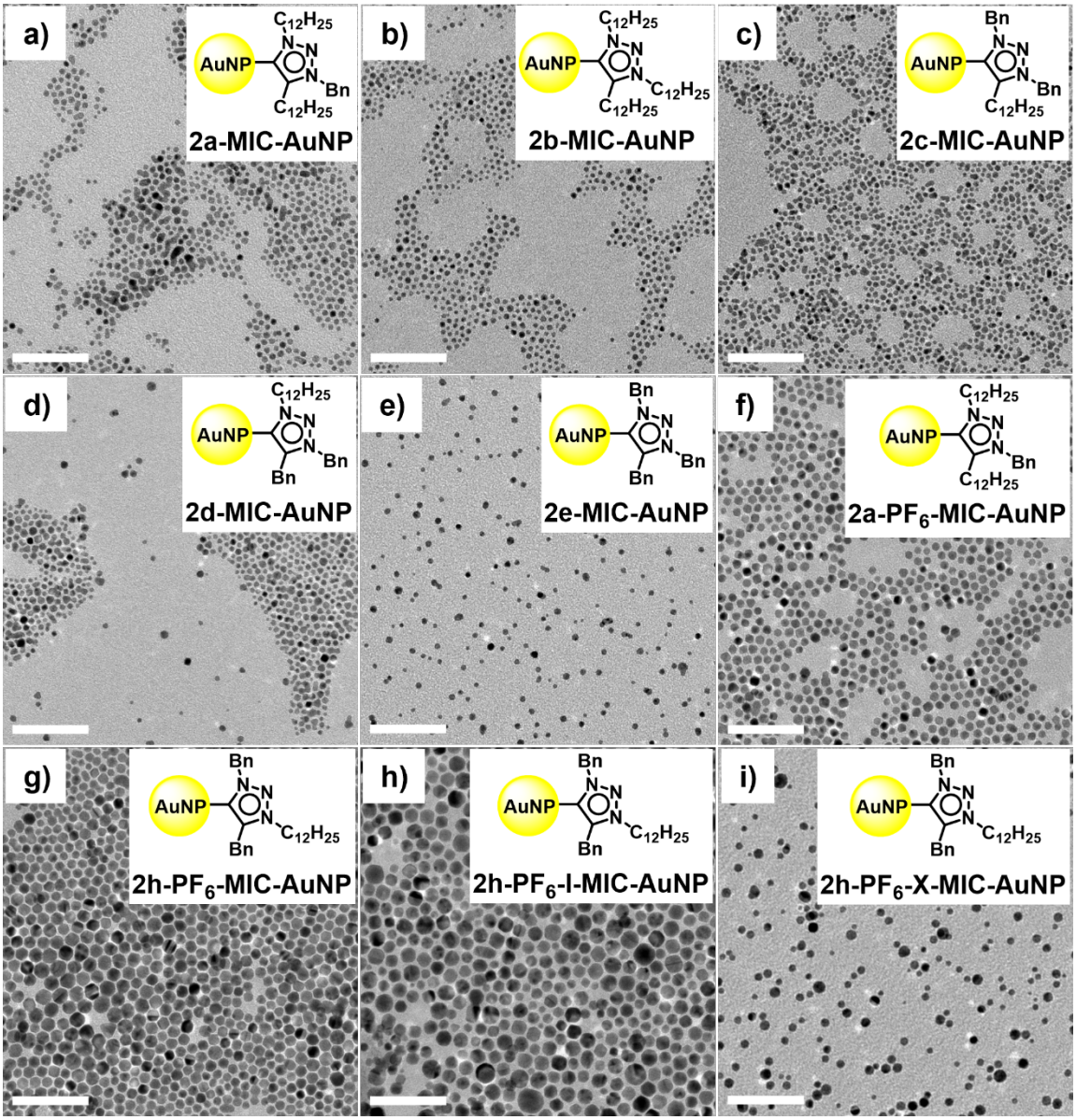


**Figure 2.** TEM images of **2-MIC-AuNPs**. Scale bars are 50 nm.

**Tuning of MIC-AuNP size**

The majority of isolated MIC-AuNPs displayed very similar sizes ranging from 2.8 – 3.2 nm (Table 1). However, **2a-$PF_6$-MIC-AuNP** and **2h-$PF_6$-MIC-AuNP** demonstrate that AuNP size can be modified by the nature of the triazolium salt and its counterion (5.1 ± 0.8 and 7.4 ± 1.8 nm, Table 1 entries 3 and 9, respectively). To further investigate tuneability and control of nanoparticle size we varied the ratio of Au(III) and triazolium salt precursors. Starting with triazolium salts **2a** and **2a-$PF_6$**, no significant difference in MIC-AuNP sizes were observed by decreasing the Au/**2a** ratio to 1:1 (compared to the 1:4 ratio described above). **2a-I-MIC-AuNP** and **2a-$PF_6$-I-MIC-AuNP** exhibit sizes of 4.3 ± 1.1 and 5.2 ± 1.5 nm, respectively (Figure S2 and S8), as compared to **2a-MIC-AuNP** and **2a-$PF_6$-MIC-AuNP**, with sizes of 3.2 ± 0.6 nm and 5.1 ± 0.8 nm, respectively (Figure 2 a and g). However, modifying the Au/triazolium salt ratio with precursor **2h-$PF_6$** allowed for control of the AuNP size. Decreasing the Au/**2h-$PF_6$** ratio to 1:1 allowed isolation of **2h-$PF_6$-I-MIC-AuNP** with a larger size of 8.8 ± 2.5 nm, while increasing the ratio to 1:10 allowed isolation of **2h-$PF_6$-X-MIC-AuNP** with a smaller size of 4.7 ± 1.6 nm as observed by TEM (Table 1 entries 10 and 11, and Figure 2 h and i, also see Figure S9-11).

Together, these findings highlight the modularity of access to various ligands that can be used to stabilise AuNPs. These MIC precursors demonstrate the flexibility, and limitations, of varying lateral ($N^1$ and $C^4$) and backbone ($N^3$) substituents of differing steric character for the synthesis and isolation of stable MIC-AuNPs. Notably, the size of MIC-AuNPs can be controlled by the nature of the triazolium salt precursor as well as the Au/triazolium ratio.

**Table 1.** Average particle sizes and PRB maxima for MIC-AuNPs synthesized.

| Entry | MIC-AuNP | Size (nm)[a] | PI (%)[b] | PRB $\lambda_{max}$ (nm)[c] |
|---|---|---|---|---|
| 1 | **2a-MIC-AuNP** | 3.2 ± 0.6 | 19 | 522 |
| 2 | **2a-I-MIC-AuNP**[c] | 4.3 ± 1.1 | 26 | 524 |
| 3 | **2a-$PF_6$-MIC-AuNP** | 5.1 ± 0.8 | 16 | 524 |
| 4 | **2a-$PF_6$-I-MIC-AuNP**[c] | 5.2 ± 1.5 | 29 | 519 |
| 5 | **2b-MIC-AuNP** | 3.0 ± 0.6 | 20 | 517 |
| 6 | **2c-MIC-AuNP** | 2.8 ± 0.5 | 18 | 523 |
| 7 | **2d-MIC-AuNP** | 3.2 ± 0.8 | 25 | 524 |
| 8 | **2e-MIC-AuNP** | 3.2 ± 0.8 | 25 | 524 |
| 9 | **2h-$PF_6$-MIC-AuNP** | 7.4 ± 1.8 | 24 | 523 |
| 10 | **2h-$PF_6$-I-MIC-AuNP**[d] | 8.8 ± 2.5 | 28 | 523 |
| 11 | **2h-$PF_6$-X-MIC-AuNP**[e] | 4.7 ± 1.6 | 34 | 521 |

[a] Determined by TEM. [b] Polydispersity Index (PI) corresponds to the ratio of the standard deviation to the average size. [c] UV/Vis spectra collected using $CH_2Cl_2$ solutions. [d] Using 1.0 equivalent of

corresponding triazolium salt **2**. [e] Using 10 equivalents of corresponding triazolium salt **2**.

## XPS studies

$^1$H NMR spectroscopy performed on purified MIC-AuNP suspensions did not allow us to conclude on the nature of capping ligands (see Figure S25-26). Indeed, ligands grafted on nanoparticles are usually quite silent, especially the sites which lie the closest to the surface and, accordingly, bear the information on grafting. This feature is related to the distribution of local environments and the strong shortening of the transverse relaxation time, which is due to a decrease of the local mobility.[9,17,18] Both effects are responsible for a broadening of the signals, which finally disappear in the base line.

To gain insight into the surface structure of these nanoparticles, XPS analyses were carried out on starting triazolium salts **2a**, **2h-PF$_6$** and their corresponding MIC-AuNPs. Regarding the starting triazolium salts, analysis of each relevant photopeak (C 1s, N 1s, Br 3d, F 1s and P 2p) confirmed the expected stoichiometry for each precursor (see Figure 3, S14-15 and Table S1 for complete details including stability of samples under X-ray irradiation Figure S16).[19]

Analysis of **2h-PF$_6$-MIC-AuNP** showed the presence of carbon, nitrogen and gold, characteristic of the AuNP. Phosphorus and fluorine are not detected, indicating the absence of free ligand. The Au 4f spectrum (Figure 3) shows two peaks at 84.0 and 87.6 eV (Au $4f_{7/2}$ and Au $4f_{5/2}$, respectively) that are characteristic of spin-orbit splitting and confirm that the nanoparticle is exclusively comprised of Au(0) with no traces of Au(I) or remaining Au(III) precursor. Analysis of the N 1s spectrum evidences the absence of any trace of starting triazolium salt **2h-PF$_6$** and strongly supports that the surface is exclusively covered by MIC ligands. Further analysis of the N 1s photopeak revealed two distinct components at 401.2 and 400.2 eV in a 1:2 ratio. The low intensity component is attributed to the central β-N$^2$ atom, and the more intense component is assigned to both the α-N$^1$ and γ-N$^3$ atoms in the triazolylidene cycle (Figure 3).

To rationalize this attribution and better understand the MIC-Au interaction, further discussion is warranted. Analysis of the N 1s photopeaks for **2a** and **2h-PF$_6$** also reveals two components (in a 1:2 ratio) separated by the same energy shift of 0.9 eV (Figure 3). The presence of two components is expected due to the presence of two chemical environments of N atoms: a central atom (R$^1$–N–**N**=N–R$^2$) and two adjacent ones (R$^1$–**N**–N=**N**–R$^2$). Since **2a** and **2h-PF$_6$** differ by the chemical substituents carried by the N atoms, a weak energy binding shift (~0.4 eV) is observed for both components. Thus, the component at low binding energy (~402 eV) is attributed to the central β-N$^2$ atom of the triazolium salt while the component at high binding energy (~403 eV) is attributed to the two outer α-N$^1$ and γ-N$^3$ atoms that carry the positive charge.

.

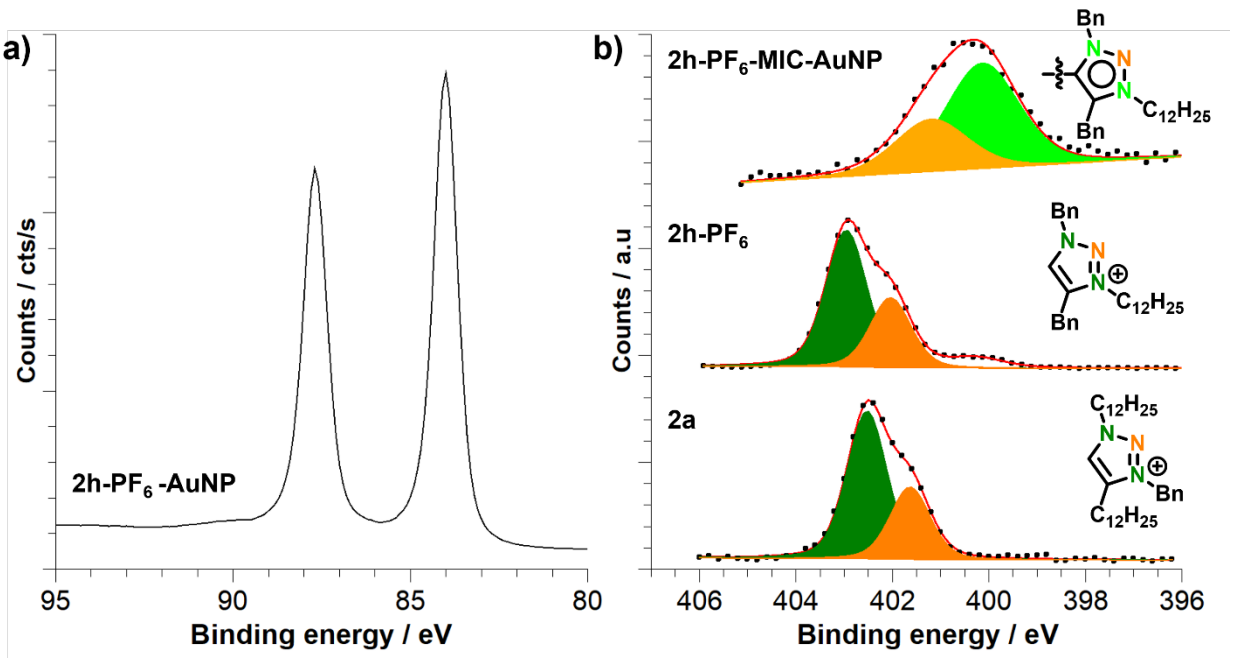


**Figure 3.** XPS spectra of **a)** Au 4f for **2h-$PF_6$-MIC-AuNP** and **b)** N 1s for **2h-$PF_6$-MIC-AuNP** (top), **2h-$PF_6$** (middle) and **2a** (bottom).

These observations allow us to suggest the following: upon formation of the MIC and consequent MIC-AuNP covalent bond there is a global loss of charge in the cycle, which results in a significant change in the N 1s binding energy ($\Delta E_b$ = -2.7 eV) of the N atoms that previously carried the positive charge (α-$N^1$ and γ-$N^3$). Notably, the central β-$N^2$ is practically unaffected by these electronic modifications. We have previously demonstrated the same phenomenon when comparing an imidazolium salt to its corresponding NHC-AuNP, with a significant shift of the N 1s binding energy ($\Delta E_b$ = -1.4 eV).[17]

**Stability studies**

The thermal and chemical stability of AuNPs is an important aspect for these materials depending on their targeted application. In this context, **2a-MIC-AuNP** was evaluated as a model material. The stability of the samples was studied by monitoring any changes in the PRB by UV/Vis spectroscopy that are indicative of AuNP aggregation (red shift, decrease in peak intensity, peak broadening). Gold nanoparticles from **2a-MIC-AuNP** were found to be exceptionally stable to a high concentration of exogenous thiol (10 mM DDT in $CH_2Cl_2$) over several days (Figure 4). After an initial 5% decrease in peak intensity after 5 minutes exposure, decreases in peak intensity are marginal with only a 10% and 14% decrease after 24 hours and 5 days, respectively. Importantly, only changes in peak intensity are observed without red shift of the PRB maximum or ripening. Exceptionally, TEM analysis of nanoparticles after 24 hours in the thiol solution shows that they maintain their spherical shape and present an identical

size to the starting material (3.3 ± 0.6 nm, see Figure S20). Additionally, a sample at the 24-hour time-point was also analysed by XPS. As expected, the characteristic signals of **2a-MIC-AuNP** were observed (C 1s, N 1s and Au 4f). However, a weak doublet at 162.0 and 163.2 eV was observed (see Figure S21) indicating the presence of sulfur.[20] Notably, due to the inconsistency in the expected peak area ratio between the S $2p_{3/2}$ and the S $2p_{1/2}$ peaks (theoretically 0.5) for sulfur covalently bound to gold, the attribution of this doublet to the presence of free thiol cannot be excluded (binding energy 163.6 and 164.9 eV for S $2p_{3/2}$ and S $2p_{1/2}$, respectively) and can be estimated to be 25% of the total measured sulfur. Therefore, due to the low amount of sulfur detected by XPS (S 2p/N 1s = 0.13), it is difficult to conclude whether substitution of MIC has occurred, or this is simply the adsorption of traces of DDT on “non-occupied” surface sites on the nanoparticle. The stability observed by UV/Vis and TEM studies, would seem to support the latter.

Thermal stability was evaluated by dispersing **2a-MIC-AuNP** in toluene and exposing the solution to various conditions. The nanoparticles showed high thermal stability, with almost no degradation observed after 24 hours at -18 °C (Figure 4 b). Additionally, heating the same sample at 110 °C did not show any signs of degradation, the PRB band only slightly sharpened with no loss in intensity or significant shift in the $\lambda_{max}$ of the PRB (Figure 4 b). These observations indicate that ripening is occurring to a certain degree without any degradation,[21] as confirmed by TEM analysis (3.8 ± 1.4 nm, see Figure S23). Significant degradation, evidenced by a decrease in peak intensity, was only observed when the nanoparticles were heated at 150 °C for 24 hours. Although the nanoparticles maintained their spherical shape, they doubled in size (6.4 ± 1.8 nm, see Figure 4 b and Figure S24).

Importantly, these results demonstrate that MIC-AuNPs outperform their NHC counterparts that show complete degradation in the presence of exogenous thiols within 24 hours.[10d,f] Notably, the stability of MIC-AuNPs resembles that of bidentate NHC-AuNPs reported by Crudden.[22] These results combined, demonstrate the exceptional stability MIC ligands impart to AuNPs, evidencing the increased σ-donation of MICs and therefore stronger ligand-surface metal interaction. Such a high stability to exogenous thiols has also been reported by Nazemi with AuNPs stabilized by polymeric MIC ligands.[15]

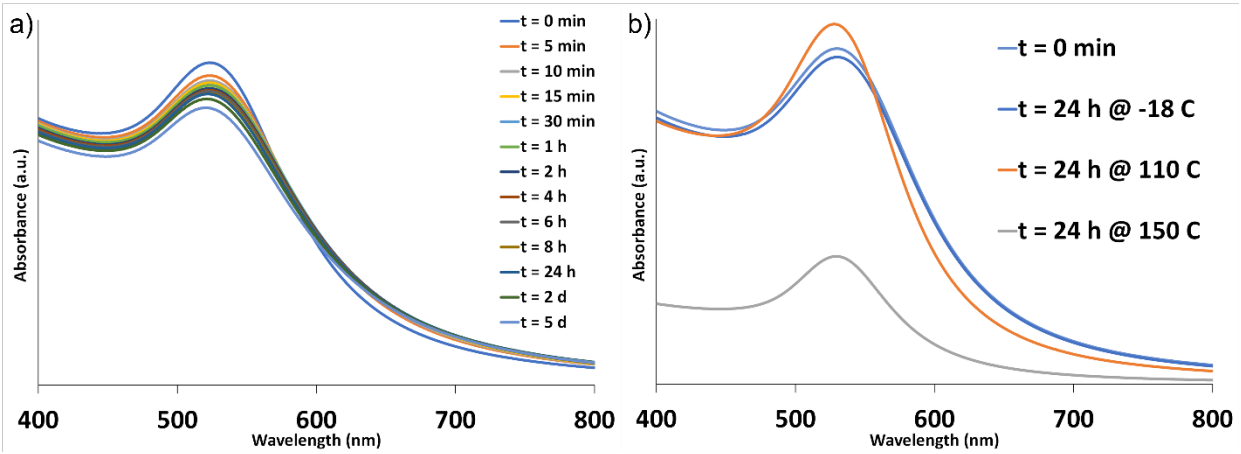


**Figure 4.** UV/Vis spectra of a) **2a-MIC-AuNP** in 10 mM DDT in $CH_2Cl_2$ and b) **2a-MIC-AuNP** in toluene at various temperatures.

**Insights on the reaction mechanism**

To gain insight into the mechanism of MIC-AuNP formation we synthesized MIC-Au(I) (**3a**) and MIC-Au(III) (**3a'**) chloride complexes from triazolium bromide **2a** following known protocols (Scheme 3).[23] The isolated complexes **3a** and **3a'** were subjected to the same NP synthetic protocol, in the absence of now redundant NaH, used for **2-MIC-AuNP**. Intriguingly, under otherwise identical conditions, the reduction step and consequent formation of NPs using molecular Au(I) and Au(III) chloride complexes, **3a** and **3a'**, was significantly slower than in the one-pot method described above with triazolium bromide **2a** (10-15 minutes vs. instantaneous, respectively). This was qualitatively observed by the time taken for the reaction mixture to turn deep burgundy red, indicating formation of MIC-AuNPs.

The isolated nanoparticles, **3a-MIC-AuNP**, presented a slightly red-shifted PRB at 536 nm compared to **2a-I-MIC-AuNP** (524 nm). TEM analysis of **3a-MIC-AuNP** showed that spherical nanoparticles are obtained with a size of 5.0 ± 1.2 nm (see Figure S12), which is very similar to the size of **2a-I-MIC-AuNP** (4.3 ± 1.1 nm). While nanoparticles **3a'-MIC-AuNP** presented an even more red-shifted PRB at 549 nm, with a similar size of 5.9 ± 0.9 nm (see Figure S13). Additionally, suspensions of **3a-MIC-AuNP** and **3a'-MIC-AuNP** in $CH_2Cl_2$ were stable for months. These findings suggest that MIC-Au(I) complexes are viable precursors,[15] and importantly also demonstrate that MIC-Au(III) complexes can be used. However, the difference in reaction kinetics observed between the one-pot process and reduction of the molecular complexes suggests that alternative mechanisms are likely at play. Moreover, the direct synthesis reported here with triazolium salts, which react faster, does not seem to involve an *in situ* generated MIC-Au(III)$Cl_3$ complex.

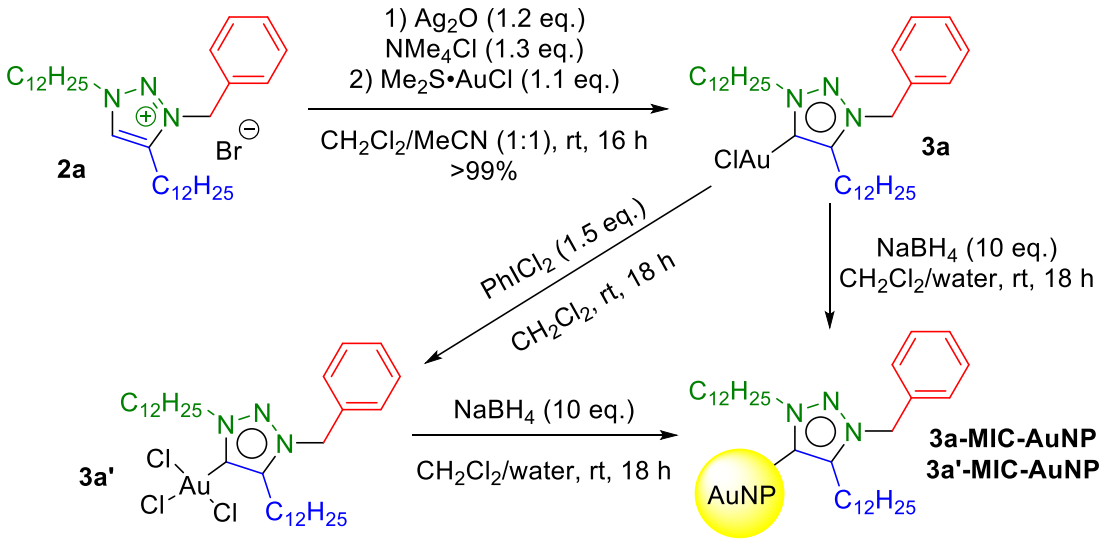


**Scheme 3**. Synthesis of MIC-Au(I) and Au(III) chloride complex **3a** and **3a'** and the corresponding **3a/3a'-MIC-AuNPs**.

## Conclusion

The use of 1,2,3-triazolium salts, as a platform for MIC ligand precursors, allows the synthesis and stabilization of gold nanoparticles of controllable size, as exemplified in this work. Rich structural diversity of ligands is easily attainable by leveraging the modularity of the CuAAC reaction. Additionally, the procedure for nanoparticle synthesis is simple, involving a one-pot protocol from triazolium salt to MIC-AuNP under mild conditions. In contrast to previous protocols, this method obviates the need to pre-isolate and purify MIC-Au(I) complexes. This strategy works with a series of triazolium salts to give stable MIC-AuNPs whose size can be controlled by the nature of the ligand as well as the Au/ligand ratio.

The exceptional stability of these MIC-AuNPs was demonstrated against exogenous thiols and harsh thermal conditions. Mechanistic studies were undertaken proving that both MIC-Au(I) and Au(III) complexes are viable precursors to nanoparticles, although the actual underlying mechanism most likely involves other processes.

Thus far, essentially thiols and ImNHCs have been used to stabilize Au nanoparticles. Here, we demonstrate that MICs, based on the 1,2,3-triazol-5-ylidene scaffold, have proven to be strong stabilizing ligands and allow the isolation of AuNPs. This original protocol will allow access to new possibilities regarding nanoparticle functionalisation and will allow further developments towards diverse application of these novel materials.

**Acknowledgements**
The authors acknowledge Sorbonne Université, CNRS and IUF for financial support and the SM3 platform of SU for high-resolution mass spectrometry analysis. This work was supported by the Initiative pour les Sciences et l'Ingénierie Moléculaires de l'Alliance Sorbonne Université in the frame of the project MIC-Au. This work has been supported by the French National Agency (ANR) in the frame of the project COCOsMEN (ANR-18-CE09-0002).

**Keywords:**
carbene ligands • gold nanoparticles • mesoionic carbenes • photoelectron spectroscopy • triazolium

**References**

[1] a) Nanoparticles: From theory to applications, G. Schmidt (Ed.), Wiley-VCH, 2nd edition, **2010**; b) W.J. Stark, P.R. Stoessel, W. Wohlleben, A. Hafner, *Chem. Soc. Rev.* **2015**, *44*, 5793-5805; c) M.J. Mitchell, M.M. Billingsley, R.M. Haley, M.E. Wechsler, N.A. Peppas, R. Langer, *Nat. Rev. Drug. Disc.* **2021**, *20*, 101-124.

[2] Gold Nanoparticles for Physics, Chemistry and Biology, C. Louis, O. Pluchery (Eds.), World Scientific, 2nd edition, 2017.

[3] a) S. Her, D.A. Jaffray, C. Allen, *Adv. Drug. Deliv. Rev.* **2017**, *109*, 84-101; b) S. Zeng, K.T. Yong, I. Roy, X.Q. Dinh, X. Yu, F. Luan, *Plasmonics* **2011**, *6*, 491-506; c) E.C. Dreaden, A.M. Alkinaly, X. Huang, C.J. Murphy, M.A. El-Sayed, *Chem. Soc. Rev.* **2012**, *41*, 2740-2779; d) M.-C. Daniel, D. Astruc, *Chem. Rev.* **2004**, *104*, 293-346.

[4] a) A.V. Zhukhovitskiy, M.J. MacLeod, J.A. Johnson, *Chem. Rev.* **2015**, *115*, 11503-11532; b) C.A. Smith, M.R. Narouz, P.A. Lummis, I. Singh, A. Nazemi, C.-H. Li, C.M. Crudden, *Chem. Rev.* **2019**, *119*, 4986-5056; c) Y.-Y. An, J.-G. Yu, Y.-F. Han, *Chin. J. Chem.* **2019**, *37*, 76-87.

[5] a) C. M. Crudden, J. H. Horton, I. I. Ebralidze, O. V Zenkina, A. B. McLean, B. Drevniok, Z. She, H. Kraatz, N. J. Mosey, T. Seki, E. C. Keske, J. D. Leake, A. Rousina-Webb, G. Wu, *Nat. Chem.* **2014**, *6*, 409–414; b) L. M. Sherman, S. L. Strausser, R. K. Borsari, D. M. Jenkins, J. P. Camden, *Langmuir* **2021**, *37*, 5864–5871.

[6] A. Bakker, M. Freitag, E. Kolodzeiski, P. Bellotti, A. Timmer, J. Ren, B. Schulze Lammers, D. Moock, H. W. Roesky, H. Mönig, S. Amirjalayer, H. Fuchs, F. Glorius, *Angew. Chem. Int. Ed.* **2020**, *59*, 13643–13646.

[7] a) M.N. Hopkinson, C. Richter, M. Schedler, F. Glorius, Nature 2014, 510, 485-496; b) H.V. Huynh, *Chem. Rev.* **2018**, *118*, 9457-9492.

[8] E.C. Hurst, K. Wilson, I.J.S. Fairlamb, V. Chechik, *New J. Chem.* **2009**, *33*, 1837-1840.
[9] J. Vignolle, T.D. Tilley, *Chem. Commun.* **2009**, 7230-7232.
[10] For recent and leading references, see: a) C. J. Serpell, J. Cookson, A. L. Thompson, C. M. Brown, P. D. Beer, *Dalton Trans.* **2013**, *42*, 1385–1393; b) J. Crespo, Y. Guari, A. Ibarra, J. Larionova, T. Lasanta, D. Laurencin, J. M. López-De-Luzuriaga, M. Monge, M. E. Olmos, S. Richeter, *Dalton Trans.* **2014**, *43*, 15713–15718; c) A. Ferry, K. Schaepe, P. Tegeder, C. Richter, K. M. Chepiga, B. J. Ravoo, F. Glorius, *ACS Catal.* **2015**, *5*, 5414–5420; d) M. J. MacLeod, J. A. Johnson, *J. Am. Chem. Soc.* **2015**, *137*, 7974–7977; e) M. R. Narouz, C.-H. Li, A. Nazemi, C. M. Crudden, *Langmuir* **2017**, *33*, 14211–14219; f) K. Salorinne, R. W. Y. Man, C.-H. Li, M. Taki, M. Nambo, C. M. Crudden, *Angew. Chem. Int. Ed.* **2017**, *56*, 6198–6202; g) A. J. Young, M. Sauer, G. M. D. M. Rubio, A. Sato, A. Foelske, C. J. Serpell, J. M. Chin, M. R. Reithofer, *Nanoscale* **2019**, *11*, 8327–8333; h) N. A. Nosratabad, Z. Jin, L. Du, M. Thakur, H. Mattoussi, *Chem. Mater.* **2021**, *33*, 921–933.
[11] G. M. D. M. Rúbio, B. K. Keppler, J. M. Chin, M. R. Reithofer, *Chem. - A Eur. J.* **2020**, *26*, 15859–15862.
[12] Z.G. Wu, X.J. Liao, L. Yuan, Y. Wang, Y.X. Zheng, J.L. Zuo, Y. Pan, Y. *Chem. - A Eur. J.* **2020**, *26*, 5694–5700.
[13] M. Albrecht, *Chimia* **2009**, *63*, 105-110.
[14] G. Guisado-Barrios, M. Soleilhavoup, G. Bertrand, *Acc. Chem. Res.* **2018**, *51*, 3236–3244.
[15] During the preparation of this manuscript a related report on MIC stabilized AuNPs was published: D.T.H. Nguyen, M. Bélanger-Bouliga, L.R. Shultz, A. Maity, T. Jurca, A. Nazemi, *Chem. Mater.* **2021**, *33*, 24, 9588-9600.
[16] a) L. Hippolyte, New syntheses of N-heterocyclic carbene-stabilized gold nanoparticles, Doctoral dissertation, Sorbonne Université, **2018**; b) A. Porcheron, Plasmonic nanoparticles modified by coordination complexes, Doctoral dissertation, Sorbonne Université, **2021**.
[17] N. Bridonneau, L. Hippolyte, D. Mercier, D. Portehault, M. Desage-El Murr, P. Marcus, L. Fensterbank, C. Chanéac, F. Ribot, *Dalton Trans.* **2018**, *47*, 6850–6859.
[18] a) J. Crespo, Y. Guari, A. Ibarra, J. Larionova, T. Lasanta, D. Laurencin, J. M. Lopez-de-Luzuriaga, M. Monge, M. E. Olmos and S. Richeter, *Dalton Trans*. **2014**, *43*, 15713; b) P. Lara, O. Rivada-Wheelaghan, S. Conejero, R. Poteau, K. Philippot and B. Chaudret, *Angew. Chem. Int. Ed.* **2011**, *50*, 12080–12084; c) C. Goldmann, F. Ribot, L. F. Peiretti, P. Quaino, F. Tielens, C. Sanchez, C. Chanéac, D. Portehault, *Small* 2017, *13*, 1604028.

[19] An important experimental factor we observed that merits mention is that the counter ion plays a key role in the stability of the triazolium salt precursor under X-ray irradiation. During experiments an evolution of the N 1s signal is observed with the emergence of a new component at a lower binding energy. This effect was significant for **2a** while only trace modifications to spectra were observed using **2h-$PF_6$** (see the ESI for details).
[20] A.-L. Morel, R.-M. Volmant, C. Méthivier, J.-M. Krafft, S. Boujday, C.-M. Pradier, *Colloids Surfaces B Biointerfaces* **2010**, *81*, 304–312.
[21] P. Sahu, B. L. V Prasad, *Langmuir* **2014**, *30*, 10143–10150.
[22] R. W. Y. Man, C.-H. Li, M. W. A. MacLean, O. V. Zenkina, M. T. Zamora, L. N. Saunders, A. Rousina-Webb, M. Nambo, C. M. Crudden, *J. Am. Chem. Soc.* **2018**, *140*, 1576–1579.
[23] a) R. Pretorius, M. R. Fructos, H. Müller-Bunz, R. A. Gossage, P. J. Pérez, M. Albrecht, *Dalton Trans.* **2016**, *45*, 14591–14602; b) M. Navarro, A. Tabey, G. Szalóki, S. Mallet-Ladeira, D. Bourissou, *Organometallics* **2021**, *40*, 1571–1576.